Direct measurements of the penetration depth in a superconducting film using magnetic force microscopy

E. Nazaretski,[1,2] J. P. Thibodaux,[3] I. Vekhter,[3] L. Civale,[1] J. D. Thompson,[1] and R. Movshovich[1]

[1]*Los Alamos National Laboratory, Los Alamos, NM 87545*
[2]*Brookhaven National Laboratory, Upton, NY 11973*
[3]*Department of Physics and Astronomy, Louisiana State University, Baton Rouge, LA 70803*

We report the local measurements of the magnetic penetration depth λ in a superconducting Nb film using magnetic force microscopy (MFM). We developed a method for quantitative extraction of the penetration depth from single-parameter simultaneous fits to the lateral and height profiles of the MFM signal, and demonstrate that the obtained value is in excellent agreement with that obtained from the bulk magnetization measurements.

A fundamental property of superconductors is the ability to expel an external magnetic field (Meissner effect), which is screened on the scale of the magnetic penetration depth, λ. In type II superconductors above a lower critical field (H_{c1}), however, it is energetically favorable to allow partial penetration of the magnetic field in quantized units called vortices. Each vortex carries one flux quantum, Φ_0, and is surrounded by supercurrents, which, in the dilute vortex limit, decay on the same length scale, λ. The value of λ is related to the density of the superconducting electrons, and its quantitative determination is important for understanding of superconducting materials, symmetry of the superconducting state and underlying mechanism of superconductivity. [1, 2, 3, 4] Experimental techniques that measure λ in bulk samples include microwave measurements [5, 6], microstrip resonators [7], two-coil mutual inductances [8], muon-spin-rotation [9] and superconducting quantum interference device (SQUID) magnetometry. [10] Recently, scanning probes have been applied to in-situ measurements of λ. Scanning SQUID [11] and scanning Hall microscopy [12] measure the vortex magnetic field above the surface of a sample, but the data analysis needs to take into account many parameters, and multistep lithography is required for the optimized performance and sensitivity of both probes. [13, 14, 15]

Magnetic Force Microscopy (MFM), a well established scanned probe technique, has been used for imaging and manipulation of individual vortices in thin films and single crystals [16, 17, 18, 19], but, until now, MFM has not been implemented for measurements of the absolute values of λ due to complexity of acquired images. Roseman et al. [20] estimated the penetration depth from the width of the lateral constant height scans of the magnetic force across a vortex, treating the tip as a point object, and found the value of λ several times higher than that obtained by other methods. In this Letter, we report the measurements of the absolute value of λ using the MFM technique. We use the knowledge of the size and magnetic properties of the probe tip to develop a model that allows us to fit the acquired MFM spectra with the penetration depth λ as the only fitting parameter. We compare obtained best fitting values of λ, with those measured in a SQUID magnetometer, and demonstrate that our experimental and modeling approach allows for the extraction of the penetration depth from the MFM measurements on an individual vortex.

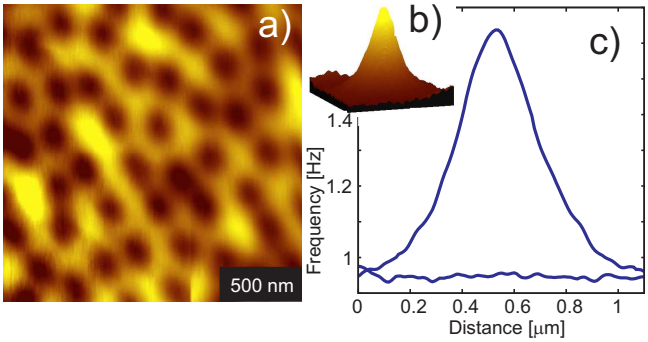

FIG. 1: (Color online) a) 1.9×1.9 μm^2 scan in a Nb film at 4.3 K. The field of view contains 53 vortices, and the vortex density agrees well with the expected value in 30 mT field. b) image of an individual vortex acquired in the external field of 1 mT, the color scale corresponds to 0.7 Hz cantilever resonance frequency change which is a function of the field above the vortex c) cross section of the vortex and the background noise.

All measurements described in this Letter were performed in a home-built low temperature MFM apparatus at T = 4.3 K. Details of the experimental setup can be found in Ref. [21]. We imaged vortices in a 300±5 nm thick niobium film fabricated by electron beam deposition. With a tip-sample distance of $\sim$ 25 μm, the sample was cooled through T_c (T_c = 8.6 K measured with the SQUID magnetometer) to 4.3 K in the presence of a magnetic field. The tip was then brought close to the sample for imaging in the dynamic MFM mode. We used high resolution SSS-QMFMR cantilever with a resonant frequency of $f_0 \sim 70$ kHz and a spring constant of $c = 1.6$ N/m available from Nanosensors Inc. (www.nanosensors.com). Fig. 1 demonstrates imaging of vortices in the Nb film with panel a) taken in the sample cooled in a field of 30 mT, and panel b) giving the profile of an individual vortex imaged in the field of 1 mT (yielding large intervortex spacing). It is important to

mention that standard MFM cantilevers have difficulties resolving individual vortices in fields higher than 10 mT [17] and an ultra-sharp double-pyramid design of MFM tips has been used in our probes. Panel c) shows the cross section of the vortex, and is a typical curve used for fitting below. We also recorded MFM spectra as a function of the probe-sample separation.

The measured frequency shift,

$$\Delta f = \frac{f_0}{2c}\frac{\partial F_z}{\partial z}\,, \tag{1}$$

depends on the force on the cantilever due to the spatially varying magnetic field of the vortex. At each point with a local magnetic moment $\mathbf{m}(\mathbf{r})$, the force $\mathbf{F}(\mathbf{r}) = \nabla[\mathbf{m}(\mathbf{r}) \cdot \mathbf{B}(\mathbf{r})]$, so that the net force on the tip is

$$\mathbf{F} = \int_{tip} \nabla[\mathbf{m}(\mathbf{r}) \cdot \mathbf{B}(\mathbf{r})] d\mathbf{r}\,. \tag{2}$$

Previous work showed that, if the tip is treated as a point object, the resulting value of the penetration depth is nearly two times larger than expected [20]. Consequently, we parameterize the tip as two cones as shown in the inset of Fig. 2 d), based on scanning electron microscope images of a tip. The tip is covered with a magnetic Co-Cr film of thickness 12 nm, and the film is saturated in an external field prior to measurements to the saturation magnetization of $M_{sat} \approx 0.8$ T [22], which gives the magnetic moment per unit volume of 6.4×10^5 A/m.

Since the thickness of the superconducting sample is several times the penetration depth (the assumption confirmed by the value of λ we find below), the field at distance z above the film surface is very close to that of the vortex outside of a bulk superconductor, and is very well approximated by the field of a magnetic monopole of magnitude $2\Phi_0$, where Φ_0 is located at distance d below the surface [23]. The far, $z \gg \lambda$ (near, $z \leq \lambda$) field is best described by $d = \lambda$ ($d = 1.27\lambda$) [23], and we use the interpolation formula $d = \lambda(1 + 0.27/(1 + z^2/\lambda^2))$ in our fitting procedure. Importantly, with this interpolation, the penetration depth is the only fitting parameter.

The fits to the MFM scans are shown in Fig. 2, and demonstrate that $\lambda_f = 109$ nm gives a high quality agreement with the experimental results. To obtain this value we used the Levenberg-Marquardt nonlinear least squares fitting algorithm [24], where the variance of the experimental data relative to the best fit is $\sigma_e^2 = N^{-1}\sum_i (f_i - f_m(x_i, \lambda_f))^2$, where f_m is the model prediction for a given data point (x_i) and f_i is the experimental data point. Fig. 3 shows the measure of the fit quality, $\chi^2 = (N\sigma_e^2)^{-1}\sum_i (f_i - f_m(x_i, \lambda_f))^2$, so that $\chi^2 \approx 1$ means a good fit. The deeper minimum in Fig. 3 b) indicates that the vertical scan is more restrictive for our fitting procedure. Consequently, the simultaneous fit to both scans yields $\lambda_f = 109 \pm 11$ nm, with the variance $\sigma_\lambda^2 = \sigma_e^2 \sum_i \left(\frac{\partial f_m(x_i,\lambda)}{\partial \lambda}\right)^{-2}$. This value exceeds the penetration depth for pure Nb, $\lambda_0 = 39$ nm, likely due to the presence of disorder, see below.

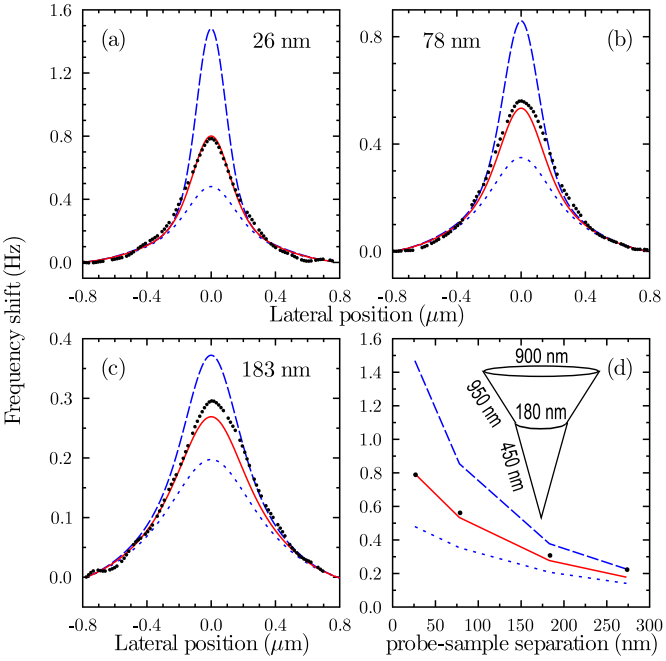

FIG. 2: (Color online) Comparison of the model to the experimental data (dots) for lateral scans, a)-c), and the probe-sample separation (vertical) scans, d). $\lambda = 60, 109, 160$ nm correspond to dotted, solid, and the dashed lines respectively. The probe-sample distance is indicated in each panel.

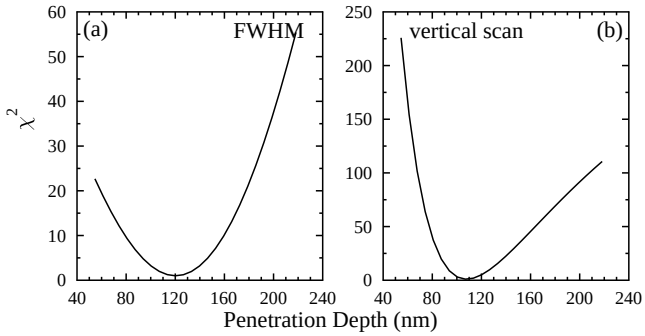

FIG. 3: Fit quality χ^2 for the full width half maximum (FWHM) of the a) lateral scan and for the b) vertical scan for 26, 78, 183, and 273 nm probe-sample separations.

We used a SQUID magnetometer to verify our result for λ by dc magnetization. Measurements were performed on a 5x3 mm^2 Nb film with the field applied normal to the surface. A typical magnetization hysteresis loop M(H), obtained at T = 4.5 K after cooling the sample from above T_c in zero field, is shown in Fig. 4. H_{c1} cannot be used for a reliable determination of λ since demagnetization effects in this configuration are large and the vortex penetration field is strongly increased by pinning. In contrast, the measurement determines the upper critical field, $H_{c2} = \Phi_0/2\pi\xi^2(T)$ (marked by the vertical

arrow in Fig. 4), where ξ is the superconducting coherence length. We fit H_{c2}(T) with a straight line with $T_c = 8.6$ K and the slope $dH_{c2}/dT = -3200$ Oe/K. Using the dirty limit results $\xi(T) = 0.855\sqrt{\xi_0 l/(1-T/T_c)}$, and $\lambda(T)$=$\lambda_0(T)$ $\sqrt{(\xi_0/1.33l)}$ [25] with the clean Nb values $\xi_0 = 38$ nm and $\lambda_0 = 39$ nm, we obtain the electronic mean free path $l \approx 4.2$ nm and $\lambda(0) \approx 102$ nm (thus $\lambda(4.3\text{K}) \approx 105$ nm), in excellent agreement with the MFM fits above.

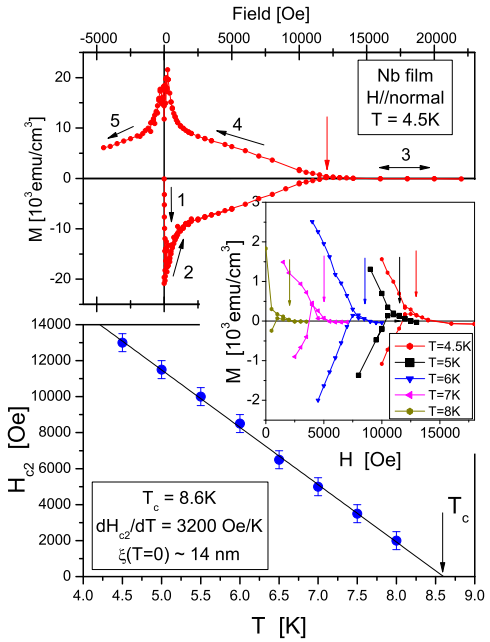

FIG. 4: (Color online) Measurements of the dc magnetization in the Nb film. Top panel: Hysteresis loop. Segment 1 is the Meissner response, segments 2 and 4 are in the vortex state, with hysteresis due to pinning. The vortex signal disappears along segment 3, above the upper critical field H_{c2}. Middle panel: expanded high field region used for determination of H_{c2} at different temperatures. Bottom panel: temperature dependence of $H_{c2}(T)$

To conclude, we have developed a method for reliable extraction of the numerical values of λ from MFM images of vortices in superconducting films. We demonstrated the viability of the method by studying the Nb film. We expect that this approach will be used for *local* determination of the penetration depth in a variety of novel superconductors and opens new avenues for the application of MFM in *quantitative* studies of materials.

We acknowledge technical assistance of J. K. Baldwin with fabrication of Nb films. This work was supported by the US DOE at Los Alamos and via Grant No. DE-FG02-08ER46492 (I. V. and J. P. T.), by the Louisiana Board of Regents (J. P. T.), and was performed, in part, at the Center for Integrated Nanotechnologies at Los Alamos and Sandia National Laboratories.

[1] R. Prozorov, R. W. Giannetta, P. Fournier and R. L. Greene, Phys. Rev. Lett. **85**, 3700 (2000).
[2] I. Bonalde, Brian D. Yanoff, M. B. Salamon, D. J. Van Harlingen, E. M. E. Chia, Z. Q. Mao and Y. Maeno, Phys. Rev. Lett. **85**, 4775 (2000).
[3] W. N. Hardy, D. A. Bonn, D. C. Morgan, R. Liang and K. Zhang, Phys. Rev. Lett. **70**, 3999 (1993).
[4] N. Schopohl and O. V. Dolgov, Rev. Lett. **80**, 4761 (1997).
[5] W. N. Hardy, S. Kamal, and D. A. Bonn, in *The Gap Symmetry and Fluctuations in High-Tc Superconductors*, edited by J. Bok, G. Deutscher, D. Pavuna, and S. A. Wolf, Plenum, New York, 1998.
[6] C.P. Bidinosti and W.N. Hardy, Rev. Sci. Instrum. **71**, 3816 (2000).
[7] B.W. Langley, S. M. Anlage, R. F. W. Pease, and M. R. Beasley, Rev. Sci. Instrum. **62**, 1801 (1991).
[8] A. T. Fiory, A. F. Hebard, P. M. Mankiewich and R. E. Howard, Appl. Phys. Lett. **52**, 2165 (1988).
[9] J. E. Sonier, R. F. Kiefl, J. H. Brewer, D. A. Bonn, J. F. Carolan, K. H. Chow, P. Dosanjh, W. N. Hardy, Ruixing Liang, W. A. MacFarlane, P. Mendels, G. D. Morris, T. M. Riseman, and J. W. Schneider, Phys. Rev. Lett. **72**, 744 (1994).
[10] L. Civale and F. de la Cruz, Phys. Rev. B **36**, 3560 (1987), J.R. Thompson et al., Phys. Rev. B **41**, 7293 (1990).
[11] C. W. Hicks, T. M. Lippman, M. E. Huber, J. G. Analytis, J-H. Chu, A. S. Erickson, I. R. Fisher and K. A. Moler, arXiv:0903.5260.
[12] S. J. Bending and A. Oral, J. Appl. Phys. **81**, 3721 (1997).
[13] N. C. Koshnick, M. E. Huber, J. A. Bert, C. W. Hicks, J. Large, H. Edwards, and K. A. Moler, Appl. Phys. Lett. **93**, 243101 (2008).
[14] A. M. Chang, H. D. Hallen, L. Harriott, H. F. Hess, H. L. Kao, J. Kwo, R. E. Miller, R. Wolfe, and J. van der Zielb, Appl. Phys. Lett. **61**, 1974 (1992).
[15] J. W. Guikema, H. Bluhm, D. A. Bonn, R. Liang, W. N. Hardy, and K. A. Moler, Phys. Rev. B **77**, 104515 (2008).
[16] A. Moser, H. J. Hug, I. Parashikov, B. Stiefel, O. Fritz, H. Thomas, A. Baratoff, and H.-J. Güntherodt, Phys. Rev. Lett. **74**, 1847 (1995).
[17] A. Volodin, K. Temst, C. Haesendonck, Y. Bruynseraede, Physica B, **284** 815 (2000).
[18] M. Roseman, P. Grütter, Appl. Surf. Sci., **188** 416 (2002).
[19] O. M. Auslaender, L. Luan, E. W. J. Straver, J. E. Hoffman, N. C. Koshnick, E. Zeldov, D. A. Bonn, R. Liang, W. N. Hardy, and K. A. Moler, Nature Phys., **5** 35 (2009).
[20] M. Roseman, P. Grütter, New. J. Phys., **3** 24 (2001).
[21] E. Nazaretski, K. S. Graham, J. D. Thompson, J. A. Wright, D. V. Pelekhov, P. C. Hammel, and R. Movshovich, Rev. Sci. Instrum. (in press)
[22] T. Takahashi, N. Ikeda, M. Naoe, J. Appl. Phys., **70** 6056 (1991).
[23] G. Carneiro and E.H. Brandt, Phys. Rev. B **61**, 6370 (2000).
[24] W. H. Press, S. A. Teukolsky, W. T. Vetterling, and Brian P. Flannery, *Numerical Recipes* (Cambridge, 2007).

[25] M. Tinkham, *Introduction to Superconductivity*, McGraw, Inc. (1975).